

# Simulation of Thermophysical Processes at Laser Welding of Alloys Containing Refractory Nanoparticles

Anatoly N. Cherepanov<sup>1</sup>, Vasily P. Shapeev<sup>1</sup>, Guangxun Liu<sup>2</sup>, Lamei Cao<sup>2</sup>

<sup>1</sup>Khrstianovich Institute of Theoretical and Applied Mechanics SB RAS; Novosibirsk State University, Novosibirsk, Russia

<sup>2</sup>Beijing Institute of Aeronautical Materials, Beijing, China

Received 2012

## ABSTRACT

Mathematical model is formulated for description of thermophysical processes at laser welding of metal plates for the case when modifying nanoparticles of refractory compounds (nanopowder inoculators – NPI) are introduced into the weld pool. Specially prepared nanoparticles of refractory compounds serve here as crystallization centers, i.e. in fact they are exogenous inoculants on which surface clusters are grouped. This can be used to control the melt crystallization process and formation of its structure, and, therefore, properties of the weld seam. As an example, calculation results of the butt welding of aluminum alloy and steel plates are presented. The results of calculation and experimental data comparison are shown.

**Keywords:** Mathematical Model; Laser Welding; Nanopowder Inoculators; Crystallization Process; Calculation Results

## 1. Introduction

In the last years increasing attention has been paid to development of technology for laser welding of metal products. In this connection, development of appropriate mathematical models and numerical algorithms for their implementation is a pressing problem [1,2].

A mathematical model is developed in this work for description of thermophysical processes at laser welding of metal plates for the case when modifying nanoparticles of refractory compounds (nitrides, oxides, etc) are introduced in the molten pool. The mathematical model proposed is based on non-equilibrium birth and growth of crystal phase on the inoculants, which are the nanoparticles, with use of the Kolmogorov's theory for calculation of the solid phase fraction. At that, the homogeneous nucleation can be neglected.

## 2. Physicomathematical Model of the Process

Let us consider a steady-state process of two plates butt welding. We introduce the Cartesian coordinate system with  $x$  axis lying on the plates upper surface,  $z$  axis coinciding with the symmetry axis and direction of the laser beam operation, and  $y$  axis perpendicular to the joint. The coordinates origin lies on intersection of the beam axis and the plates upper surfaces (Figure 1). The beam moves along the joint in negative direction of  $x$  axis with constant welding speed  $v=const$ . The metal of the welded plates is protected from oxidation by an inert gas blow that carries away a part of the metal vapors. We assume the thermophysical parameters to be constant and equal to their average values in the temperature range under consideration. Due to the small concentration of the dispersed nanoparticles (~0.05% by mass), their influence on the physical parameters of the alloy can be neglected. The alloy is considered to be a binary system. With these assumptions, the three-dimensional equation of heat transfer in the weldpool and solid metal in the

moving coordinate system takes the form:

$$c_i \rho_i v \frac{\partial T}{\partial x} = \lambda_i \left( \frac{\partial^2 T}{\partial x^2} + \frac{\partial^2 T}{\partial y^2} + \frac{\partial^2 T}{\partial z^2} \right) - \delta \kappa \rho_i v \frac{\partial f_s}{\partial x} \quad (1)$$

where  $c_i$ ,  $\lambda_i$ ,  $\rho_i$  are specific heat, heat conductivity, and density of the  $i$ -th phase, respectively (indices  $i = 1, 2, 3$  denote parameters of solid, two-phase, and liquid states of the metal);  $\delta = 0$  in the melting zone;  $\delta = 1$  in the crystallization zone;  $f_s$  is a share of the solid phase;  $f_l = 1 - f_s$  is a share of liquid phase in the two-phase zone. In variant of the model used in this paper, all particles of the product in movable coordinate system move parallel to  $x$  axis with the welding speed. The process of melting is considered in Stefan problem approximation, considering the phase transition boundary to be a smooth surface, on which the conditions of thermodynamic equilibrium and heat balance are fulfilled:

$$T = T_m, \quad -\lambda_2 \frac{\partial T}{\partial n} \Big|_2 + \lambda_1 \frac{\partial T}{\partial n} \Big|_1 = \kappa \rho_1 (\mathbf{v} \cdot \mathbf{n}),$$

where  $T_m = (T_{l0} + T_s) / 2$  is fictitious melting temperature,  $T_{l0}, T_s$  are temperatures of equilibrium values of liquidus and

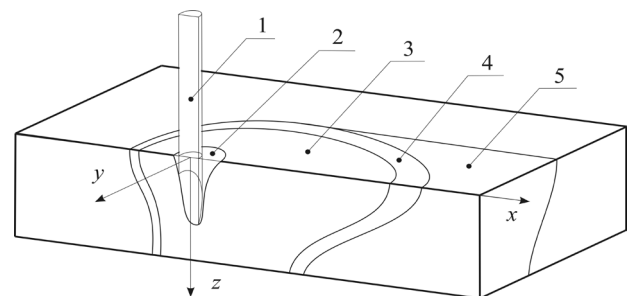


Figure 1. The weld zone layout: 1 – laser beam, 2 – steam channel, 3 – liquid phase (molten pool), 4 – two-phase zone, 5 – solid phase.

solidus, respectively,  $n$  is unit normal to the phase transition boundary,  $\kappa$  is the melting heat (heat of crystallization),  $(\lambda_1 \partial T / \partial \mathbf{n})_1$  and  $-(\lambda_2 \partial T / \partial \mathbf{n})_2$  are the heat fluxes calculated on the sides of the solid and liquid phases, respectively. This approximation is reasonable, because at high temperature gradients, zone of the phase transition at melting is a thin layer, which thickness is much less than the weld pool characteristic size. Considering  $T_m = (T_{l0} + T_s) / 2$  to be the melting temperature, we can uninterruptedly proceed to modeling of nonequilibrium heterogeneous crystallization on active superdispersed seeds in region of the alloy solidification ( $T_e \leq T < T_{l0}$ ). Here,  $T_e$  is temperature of solidification completion, determined from kinetic equation

$$T_e = T_i(C_e) - \dot{\xi}_e / K_e$$

where  $\dot{\xi}_e, C_e, K_e$  are velocity of the solidification boundary movement, impurity concentration on it, and the kinetic coefficient, respectively. For the problem's simplification, the kinetic overcooling ( $\dot{\xi}_e / K_e$ ) is neglected due to its smallness, and the temperature of solidification completion, similarly to the theory of quasi-equilibrium two-phase zone [3], is considered equal to the eutectic temperature ( $T_e = T_i(C_e)$ ), where  $C_e$  is impurity concentration in the eutectic point). In the area of solidification ( $i = 2$ ), the crystallization rate is defined by the processes of origin and growth of solid phase in overcooled alloy on seeds, which are refractory activated nanoparticles. Considering all the nanoparticles to be centers of crystallization, we can define section of the solid phase, using the formula of Kolmogorov N.E. [4,5]:

$$f_s = 1 - e^{-\Omega}, \tag{2}$$

where 
$$\Omega(x, y, z) = \frac{4\pi}{3} N_p \left( r_p + \frac{K_u}{v} \int_{x_0}^x \Delta T d\xi \right)^3$$

is volume of the crystal phase formed in overcooled melt. Here,  $N_p$  is the number of nanoparticles in volume unit;  $x_0$  is the coordinate of point  $x$  on isotherm with the temperature of liquidus  $T_{l0}$ ,  $f_i(T_{l0}) = e^{-4\pi N_p r_p^3} \approx 1$ ,  $r_p$  is the radius of nanoparticles;  $K_u$  is the constant of crystal growth in kinetic law [4-6]

$$u = K_u [T_i(C) - T]^n,$$

where  $u$  is the growth rate,  $n$  is a physical constant ( $n = 1$  at normal mechanism of growth,  $n = 2$  at dislocation one);  $T_i(C)$  is the liquidus temperature, which is approximated by linear dependence on dissolved (alloying) component  $C$ :

$$T_i(C) = T_{l0} - \beta (C - C_0),$$

where  $C_0$  is initial concentration of the dissolved component,  $\beta$  is coefficient module of the liquidus line slope on the state diagram of corresponding binary alloy,  $\Delta T$  is local overcooling, defined by equation

$$\Delta T = T_i(C) - T \tag{3}$$

According to (1), (2) and (3), in the crystallization zone ( $T_e \leq T < T_{l0}$ ) appears a source of heat, connected with heat generation during the melt crystallization. Due to nonlinear dependence of  $f_i(T)$ , contribution of this heat generation can be taken into account by solving the equation of heat conduction iteratively, specifying on iterations  $f_i$  and, consequently,  $T$  in

the zone of crystallization.

Boundary conditions. At infinite distance from the radiation source  $x \rightarrow \infty, y \rightarrow \infty$  we assume  $T(x, y, z) = T_0$ . On the plates upper and lower surfaces ( $z = 0, z = h$ ) blown by the inert gas, outside the steam channel, are fulfilled conditions of complex convective and radiation heat exchange with the environment

$$\lambda_{\Sigma m} \frac{\partial T}{\partial z} \Big|_{z=0,h} = \alpha_{\Sigma m} (T \Big|_{z=0,h} - T_0). \tag{4}$$

Here,  $T_g$  is the gas temperature,  $\alpha_{\Sigma m}$  is the total coefficient of heat transfer defined by expression

$$\alpha_{\Sigma m} = \alpha_{km} + \varepsilon_m \sigma_0 (T_{z=0}^2 + T_g^2) (T \Big|_{z=0} + T_g),$$

$\varepsilon_m$  is reduced emissivity of the heat transfer surfaces,  $m=0, 1$  for the upper and lower surfaces, respectively;  $\sigma_0$  is Stefan-Boltzmann constant,  $\alpha_{km}$  is coefficient of convective heat transfer [7]

$$\alpha_{km} = 0,646 \text{Re}_m^{1/2} \text{Pr}^{1/3} \lambda_g / l,$$

where  $\text{Re}_m = v_{gm} / \nu_g$ ;  $\text{Pr} = \nu_g / a_g$ ;  $v_{gm}$  is the gas flow velocity;  $l$  is the characteristic length of the cooling zone;  $\nu_g, a_g, \lambda_g$  are the gas kinematic viscosity, temperature conductivity, and heat conductivity, respectively.

In the laser radiation impact zone (on the steam channel surface  $z = Z_c(x, y)$ ) is fulfilled the heat balance condition:

$$-\lambda_3 \nabla T \cdot \mathbf{n} = \mathbf{q} \cdot \mathbf{n} - L \dot{m}. \tag{5}$$

Here,  $\dot{m}$  is mass velocity of the substance evaporation from the surface unit, related to the vapors excessive pressure  $P(z)$  necessary for keeping the channel walls from collapse. It is defined by relation  $\dot{m} = \sqrt{P(z)} \rho_v$ ,  $\rho_v$  is the vapor density;  $L$  is specific heat of the alloy evaporation,  $\mathbf{q}$  is the absorbed heat flux with the re-reflection taken into account,  $\mathbf{n}$  is unit normal to the channel surface. In numerical simulation, the last relation determines the heat flux on the steam channel surface and is the boundary condition for equation (1). We assume, that the welding is realized by CO<sub>2</sub> laser radiation with wavelength  $\lambda_0 = 10,6 \mu\text{m}$ . The radiation intensity is described by Gaussian normal distribution  $I(x, y, z) = I_0 \exp(-2r^2 / r_z^2)$  where  $I_0 = 2W / (\pi r_z^2)$ ;  $W$  is the laser power,  $r_z$  is the radius of the laser beam at depth  $z$  of the steam channel, determined by relation [8]

$$r_z = \sqrt{r_F^2 + \left[ \frac{z - Z_F}{\pi r_F} \lambda_0 \right]^2},$$

where  $r_F$  is the laser beam radius in focal plane;  $Z_F$  is location of the focus relative to the upper surfaces of the details welded.

For density distribution of the absorbed radiation power on the surface of the steam channel with coordinates  $z = Z_c(x, y)$  in the zone of direct interaction we have expression

$$q(x, y, Z(x, y)) = \frac{2A W}{\pi r_z^2} \exp\left(-2r^2 / r_z^2\right)$$

Here,  $A_q = A + A_e(1 - A)$  is the absorption effective coefficient. The first member in this coefficient takes into account

absorption of the radiation falling onto the surface directly from the laser beam, while the second member takes into account absorption of the radiation reflected repeatedly from the channel walls;  $A_e = A \sum_{n=1}^{\infty} [(1-A)S_b / (S_b + S_c)]^n$  value is the equivalent absorption coefficient [9],  $S_b, S_c$  are areas of lateral surface of the channel and inlet, respectively,  $A$  is coefficient of the laser radiation absorption by the steam channel surface. In the area reached by the reflected radiation only,  $A_{ef}$  lacks the first member.

### 3. Model of Steam Channel Formation

If the laser power exceeds some critical value, then in the area of the beam interaction with the metal a steam channel emerges. Even in the case of homogeneous material of the plates, and constant values of the radiation power and welding rate, its walls oscillate chaotically due to the hydrodynamic instability. The present model assumes that that channel walls oscillate by their time-averaged location. There are various models described in papers for considering the heat transfer from the beam to metal as well as approaches to calculation of the steam channel shape. Here was used a slightly modified method described in [10]. Note that the channel wall shape turns out to be similar to that of the channel front wall proposed in [11].

### 4. Numerical Method

For numerical solution of the problem about temperature distribution in the calculation domain, a known iterative finite-difference scheme of steadying for 3D heat conduction equation is used [12]. As stated above, the heat balance equations on different surfaces of the plates (4) were used as the boundary conditions. Relation (5) was taken into account on the steam channel surface. At a significant distance from the molten pool, i.e. on a remote boundary of the calculation domain, the temperature was set equal to that of the environment.

### 5. Some Results of Numerical Simulation

Some results of the temperature fields calculations in the molten pool and surrounding layers of the solid alloy are shown in the **Figure 4**. Boundaries of the pool, two-phase crystallization zone were determined from characteristic temperature values. The beam radius  $r_f$  in the focal plane was chosen as the length scale. **Figure 4** shows dimensionless temperature normalized to liquidus temperature  $T_l$ . The picture in a small part of the calculation domain is shown in the figures for the purposes of obviousness. The numerical calculations were carried out for alloy Al + 10% Si (% of mass) at the same thermophysical parameters as in [10,13]. For example, laser power  $W=3.18$  kW, welding rate  $v=4.7$  m/min, plate thickness  $h=1.5$  mm. One can see in **Figure 2** that the most warmed-up areas as well as the largest temperature gradients in calculation domain are located near the steam channel surface. One can also notice that the temperature on a sufficiently large part of front surface of the steam channel near the laser beam axis is close to the boiling-point temperature, that correlates with the channel construction method described in [10].

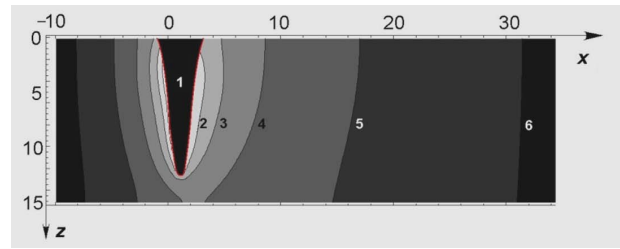


**Figure 2.** Temperature field and isotherms in calculation domain (cross-section  $y=0$ ): 1 – steam channel, 2 –  $T = 2629.1$  K (boiling-point temperature), 3 –  $T = 2155$  K, 4 –  $T = 1724$  K, 5 –  $T_{l0} = 862$  K (equilibrium liquidus temperature), 6 –  $T = 420$  K.

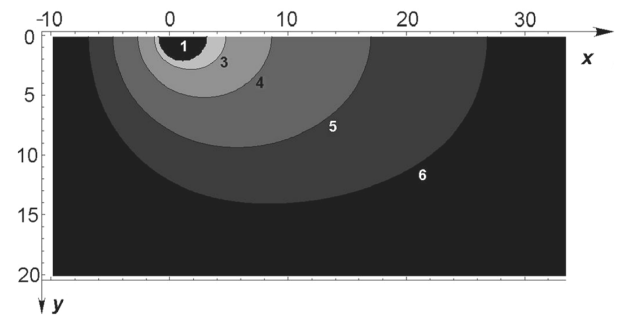


**Figure 3.** Temperature field and isotherms in calculation domain (view from above, plane  $z=0$ ): 1 – steam channel, 4 –  $T = 1293$  K, 5 –  $T_{l0} = 862$  K (equilibrium liquidus temperature), 6 –  $T=560.3$  K.

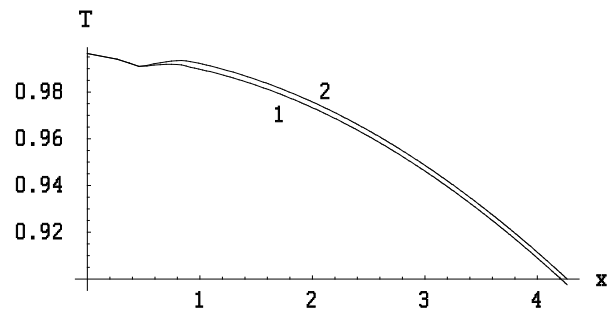


**Figure 4.** Non-dimensional temperature profile in the crystallization zone. The  $x$  axis begins at  $x_{l0}$ . Curve 1 corresponds to  $N_p = 10^{18} \text{m}^{-3}$ , curve 2  $N_p = 10^{19} \text{m}^{-3}$ .

Particularity of alloy crystallization with a modifying nanopowder is overcooling taking place in the region of emergence and growth of crystal phase, that causes non-monotony of the temperature variation along the  $x$  coordinate (**Figure 4**). Maximal value of overcooling is  $\sim 5$  K and it depends on nanoparticles quantity  $N_p$  in the melt volume unit.

Welding simulation of carbon steel plates was carried out as well. The steel chemical composition: C:0.17-0.24; Mn:0.35-0.65; Si:0.17-0.37; S:0.04; P:0.35; Ni:0.3; Cu:0.3; Cr: 0.25. The welding was performed with  $\text{CO}_2$  laser with power  $W = 5.2$  kW and 2.3 kW, the welding rate  $V_w = 2$  m/min and 0.6 m/min,  $Z_F = 0$  mm. **Figure 5(a)** shows photo of the weld seam cross-section obtained in an experiment, **Figure 5(b)** shows cross-section of this section obtained from the numerical simulation. The comparison shows satisfactory agreement between the results of calculation and experiment.

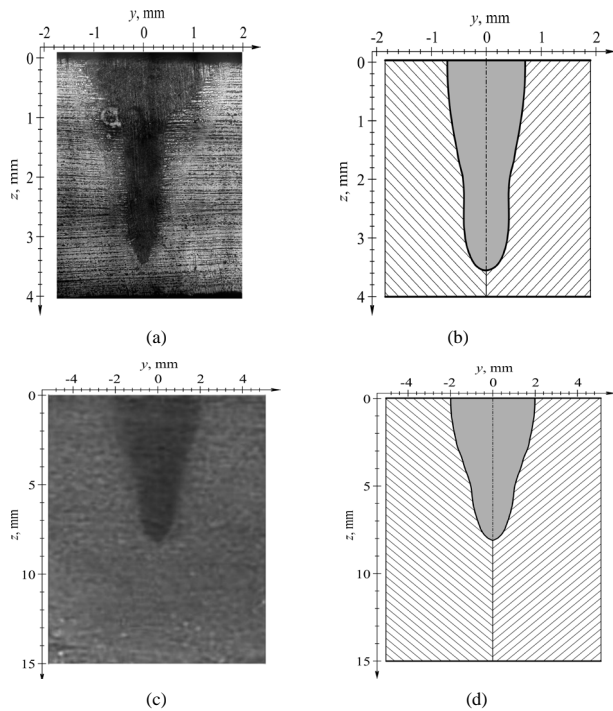


**Figure 5. Morphology comparison of cross-sections of weld seam obtained by the laser welding (a), (c) and by the numerical simulation (b), (d) at various powers of the laser radiation and the welding rate: (a), (b)  $W = 5.2$  kW,  $V = 2$  m/min; (c), (d)  $W = 2.3$  kW,  $V = 0.6$  m/min.**

## 6. Conclusions

A mathematical model of crystallization of a multi-component alloy modified by active nano-dispersed inoculators is built. It allows of analyzing influence of the inoculators concentration and their size on the structure formation processes. Particularity of heterogeneous crystallization of alloy with modifying nanopowder is appearance of overcooling in the area of birth and growth of the crystal phase. Comparison of the numerical simulation and experiment data shows satisfactory agreement of the results, that demonstrates a sufficient adequacy of the mathematical model proposed.

## 7. Acknowledgements

The work was supported by the Russian Foundation for Basic Research, project no. 10-01-00575.

## REFERENCES

- [1] Dowden J. The Theory of Laser Materials Processing. – Springer Series in Materials Science, Vol. 119, 2009.
- [2] Zhao H., White D. R., DebRoy T. Current issues and problems in laser welding of automotive aluminium alloys // *International Materials Reviews*. 1999. V. 44, № 6. P. 238–266.
- [3] Borisov V.T. Theory of two-phase zone of metallic ingots. Moscow: Metallurgiya, 1987 [In Russian].
- [4] Balandin G.F. Theory of ingot formation. Moscow: Mashinostroyeniye, 2002, 212 p. [In Russian].
- [5] A.N. Cherepanov, V.N. Popov, O.P. Solonenko. Three-dimensional crystallization of nickel drop containing refractory nanoparticles at its collision with a plate. *J. of Applied Mechanics and Technical Physics*, 2006, vol. 47, no. 1, p. 29 [In Russian].
- [6] Flemings M. Solidification processes. Moscow: Mir, 1977, 423 p. [In Russian].
- [7] Kutateladze S.S. Basics of heat exchange. Novosibirsk: Nauka, 1979, 656 p. [In Russian].
- [8] Oraevsky A.N. Gaussian beams and optical resonators // *Papers of Lebedev Physical Institute*. Moscow: Nauka, 1988. V. 187. P. 3–59 [In Russian].
- [9] Sudnik V.A., Radai D., Dorofeev V.A. Computer simulation of laser beam welding. Model and verification // *Svarochnoe pravo*. 1997. No. 1. P. 28–33 [In Russian].
- [10] Cherepanov A.N., Shapeev V.P. Numerical simulation of thin metal plates welding // *Vychislitel'nye tekhnologii*, 2009, vol. 14, no. 3, p. 96–106 [In Russian].
- [11] Xiangzhong Jin, Lijun Li, Yi Zhang. A heat transfer model for deep penetration laser welding based on an actual keyhole. *Heat and Mass Transfer*, 46 (2003) 15–22.
- [12] Yanenko N.N. The Method of Fractional Steps. Springer-Verlag, Berlin-Heidelberg-NewYork, 1971.
- [13] Cherepanov A.N., Shapeev V.P., Fomin V.M., Semin L.G. Numerical simulation of thermophysical processes at laser beam welding. *J. of Applied Mechanics and Technical Physics*. 2006. No. 5. P. 88–96 [In Russian].